International Journal of Biological Macromolecules 268 (2024) 131731

Contents lists available at ScienceDirect

International Journal of Biological Macromolecules

journal homepage: www.elsevier.com/locate/ijbiomac

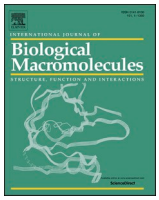

Sourcing chitin from exoskeleton of *Tenebrio molitor* fed with polystyrene or plastic kitchen wrap

Larisa Ilijin [a,*], Maria Vesna Nikolić [b], Zorka Z. Vasiljević [b], Dajana Todorović [a], Marija Mrdaković [a], Milena Vlahović [a], Dragana Matić [a], Nenad B. Tadić [c], Vesna Perić-Mataruga [a]

[a] Department of Insect Physiology and Biochemistry, Institute for Biological Research "Siniša Stanković", National Institute of Republic of Serbia, University of Belgrade, Despot Stefan Blv. 142, 11060 Belgrade, Serbia
[b] University of Belgrade - Institute for Multidisciplinary Research, Kneza Višeslava 1, 11030 Belgrade, Serbia
[c] University of Belgrade, Faculty of Physics, Studentski trg 12, 11000 Belgrade, Serbia

ARTICLE INFO

Keywords:
Chitin extraction
Characterization
Plastic biodegradation
Circular economy

ABSTRACT

In this work we have characterized and compared chitin sourced from exoskeleton of *Tenebrio molitor* larvae fed with polystyrene or plastic kitchen wrap combined with bran in the ratio 1: 1 with chitin sourced from larvae exoskeleton fed only with bran. Analysis of the frass by ATR-FTIR showed very similar spectra and confirmed degradation of the plastic feed components, while ATR-FTIR analysis of the exoskeleton verified the absence of any plastic residue. Deproteinization followed by demineralization produced 6.78–5.29 % chitin, showing that plastic (polystyrene or plastic kitchen wrap) in the larvae diet resulted in heavier insect exoskeleton, but yielded slightly less chitin, with the lowest value obtained for plastic kitchen wrap in the insect diet. The deacetylation degree of 98.17–98.61 % was determined from measured ATR-FTIR spectra. XRD analysis confirmed the presence of α-chitin with a crystallinity index of 66.5–62 % and crystallite size 4–5 nm. Thermogravimetric analysis showed similar degradation curves for all chitin samples, with two degradation steps. These results show that chitin sourced from exoskeleton of *T. molitor* larvae fed with plastic (polystyrene or plastic kitchen wrap) and contributing to significant biodegradation of major polluting materials can be a feasible and alternative source of chitin, further promoting a bio-circular economy.

1. Introduction

With global human population growth, there is an escalating demand for alternative protein rich food and livestock feed [1]. Increased costs, environmental impact, and limited availability of soybean and fish meal as currently used protein based livestock feed, have directed the search for alternative sources towards insects. Feed conversion efficacy, high nutritional quality, fast reproduction rate, sustainability of their farming even on waste streams are the reasons that have qualified inclusion of insects in farming systems. Insect farming circular, zero waste systems connect two abilities of insects: the ability to decompose waste and the ability to create high-quality nutrients, while their frass can be used as an environmentally ecofriendly fertilizer, ensuring all essential elements for plants [2], and improving plant tolerance to abiotic stress and resistance to biotic stresses [3]. Additional analysis are necessary for frass acquired from mealworms fed with plastic waste, and possible negative effects on plants due to the composition of these materials, as it was observed for spent coffee grounds derived Black Soldier Fly frass, as a result of alkaloid and caffeine present in this waste [4,5]. Insects and insect-based products for human consumption are increasing in popularity, though there are still some consumer barriers in Western countries [6,7]. Mealworm *Tenebrio molitor* (Coleoptera), an economically important species, is also one of the most examined insects in animal feed and food development research, and are successfully used in insect farming [8,9]. They serve as an alternative food source rich in proteins, lipids and polyunsaturated fatty acids in aquaculture, for pets, poultry and pigs [10,11] and increasingly in the human food industry [12,13], and represent a good solution for the large scale conversion of plant biomass into proteins.

Due to the rapid growth of the human population and increased food

* Corresponding author.
E-mail address: lararid@ibiss.bg.ac.rs (L. Ilijin).

https://doi.org/10.1016/j.ijbiomac.2024.131731
Received 27 January 2024; Received in revised form 15 March 2024; Accepted 19 April 2024
Available online 20 April 2024

consumption, the amount of organic and plastic waste is high and persistent. Plastics are a significant component of the municipal waste stream, with polystyrene (PS) and low-density polyethylene (LDPE), deriving from food packaging the most widely included plastic materials in food processing. PS is a thermoplastic styrene hydrocarbon polymer, that when rapidly heated with a foaming agent gives expanded polystyrene foam most commonly used in the food industry for protective packaging (coffee cups, food trays, etc.), and it is a major pollutant of aquatic systems (rivers, lakes, oceans) and thus marine organisms [14,15]. This plastic material is non-biodegradable and, when burnt emits polycyclic aromatic hydrocarbons and carbon monoxide, increasing the level of carbon emission [16]. The European Parliament has banned the use of expanded polystyrene foam food and drink containers from 2021. LDPE is a thermoplastic made from the monomer ethylene. LDPE is widely used as a packaging material and is highly resistant to degradation [17]. LDPE microplastic is a significant pollutant of aquatic systems and is also notably present in landfills [18,19]. It is the main component of plastic carrier bags, greenhouse plastic and kitchen plastic wrap and together with other polyethylene materials, represents up to 64 % of the synthetic plastics that are discarded within a short period after use [17]. Plastic waste is a major environmental problem and the ability of *T. molitor* larvae to biodegrade ingested plastics such as PS and LDPE, with the incorporation of waste components into insect biomass without toxic metabolic by-products, has become very attractive [20–22]. Various symbiotic bacterial strains are present in insect midgut, and besides their important role in the digestion of ingested food, some of them are capable of biodegrading different types of plastic materials. In addition to rearing these larvae as an alternative food, they may also represent the best choice as a source of chitin, the most abundant natural polymer after cellulose [23].

Structural components of the Arthropods` exoskeletons, and cell walls of fungi and yeast chitin are chitin crystalline microfibrils. Chitin represents the major constituent of the insect cuticle, and together with the protein matrix around it protects the insect from mechanical stress, dehydration, xenobiotics, and serves as attachment site for insect muscles [24]. In native state chitin is a straight chain polymer of β-1,4-*N*-acetylglucosamine, and it is present in 3 different forms: α (chains have anti - parallel orientation), β (chains have parallel orientation), and γ (sets of two parallel strands oscillate with single anti-parallel strand). In crustaceans, arthropods, including insects, the α-form is present, while the γ – form of chitin is detected in insect cocoons [25]. Chitin sources with the β-form are obtained from mollusks [26].

The majority of currently used polymers are synthetic materials. Their biocompatibility and biodegradability are much more limited than those of cellulose, chitin, chitosan, and their derivatives as naturally abundant and renewable ones. Chitin has excellent properties such as biodegradability, biocompatibility, non-toxicity, and adsorption classifying it as a relevant resource material [23]. The increased interest in chitin is also the result of numerous studies of the antimicrobial activity of lysozyme [27], as a component of the animal immune system. It disrupts bacterial cell walls and releases the chitinous material. Chitin is generally sourced from waste of the marine food industry, but chitin sourced from insects is a growingly available and stable alternative [23,28]. Chitin and especially its derivative chitosan are widely applied in the pharmaceutical and biomedical industries, cosmetics and food packaging [29–31]. Recent applications of chitin flakes or nanofibers have been for water treatment, polluting dye and heavy metal removal and in green electronics [32–34].

In this work we have sourced and compared properties of chitin obtained from exoskeleton of *T. molitor* larvae fed wheat bran, a mix of wheat bran and expanded polystyrene, as well as a mix of wheat bran and plastic kitchen wrap (mainly LDPE). We estimated the yield of isolated chitin, determined and compared the physicochemical characteristics of obtained chitins by ATR-FTIR spectroscopy, XRD, FESEM, EDS and TG/DTA. The aim was to establish, for the first time, that chitin sourced from insects consuming polluting plastics is a good and viable source, further contributing to establishment of a circular bio-economy approach and development of zero waste insect farming systems. Chitin obtained in this way can be applied in a large range of applications, or used to extract chitosan that has an even wider application potential.

2. Material and methods

2.1. Insect rearing and sample preparation

For the last three years, three self-sustaining laboratory cultures of *T. molitor*, were reared in the Department for Insect Physiology and Biochemistry on wheat bran (C-control group) and wheat bran with added polystyrene (PS group), and plastic kitchen wrap, mostly composed of low density polyethylene (LDPE group), in the ratio 1:1. Due to the lack of nitrogen in both plastic materials, larvae were not able to complete their development if fed only with plastic [21,35]. Therefore we added industrial wheat bran in the mix with the plastic material as a nutritive substrate for them. Recently, they were easily incorporated in the circular economy of insect farming (Belinda Animals, Belgrade) as the first professional insect breeding initiative in the Republic of Serbia. With optimal rearing density of 2 larvae/cm^2, the feeding rate was 1.5-2 mg of feed/larvae/day. Containers with larvae and food substrate were stored in a rearing room with constant conditions: no light, 25 °C, 70 % humidity. From all three self-sustaining *T. molitor* cultures, light yellow-brown larvae, weighing 130 to 160 mg, were randomly collected. Due to variable developmental time and number of larval instars of *T. molitor,* we picked healthy individuals with similar sizes from all three self-sustaining laboratory cultures. Larvae were sacrificed on ice, the exoskeletons were isolated: 73 from the control group, 70 from PS, and 70 from the LDPE group. They were prepared for further analysis by freeze drying for 44 h.

2.2. Attenuated total reflectance Fourier transform infrared (ATR-FTIR) spectroscopy of feedstock, frass and exoskeletons

A Fourier transform infrared spectrometer (SpectrumTwo, Perkin Elmer, Waltham, MA, USA) was used to characterize the major functional groups in the starting feedstock (industrial wheat bran - C), polystyrene (PS), plastic kitchen wrap, mostly composed of low density polyethylene (LDPE), frass and exoskeletons of *T. molitor* larvae from the C, PS and LDPE group. The frass and freeze dried larval exoskeletons were examined for traces of polystyrene and LDPE plastic. ATR-FT-IR spectra of samples were recorded directly using enough to completely cover the crystal surface. Eight scans per replicate, in the range 400–4000 cm^{-1} were recorded with a resolution of 4 cm^{-1}. For each larvae section sample two spectra were recorded. All experiments were measured in triplicate.

2.3. Chitin extraction and characterization

2.3.1. Materials

Hydrochloric acid (HCl, ACS reagent, ≥37 %, Sigma Aldrich, Merck KGaA, Darmstadt, Germany) and sodium hydroxide (NaOH pellets, 99 + % LabExpert, KEFO, Ljubljana, Slovenia) were used as received.

2.3.2. Chitin extraction

The freeze dried exoskeletons of all three groups were ground to obtain dry exoskeleton powder. It was used for two step (deproteinization and demineralization) chemical chitin extraction [36]. We applied the method described by [37,38] with some modifications (Fig. 1). In the deproteinization step the dry exoskeleton powders of all three groups were alkaline-treated with 10 % (*w*/*v*) NaOH solution at 80 °C for 24 h to remove protein, fat and color simultaneously. After centrifugation and washing with distilled water until the pH became neutral, the samples were acid-treated with 7 % (*v*/*v*) HCl solution at 25 °C for 24 h to remove minerals. In the last step, after further centrifugation and washing with

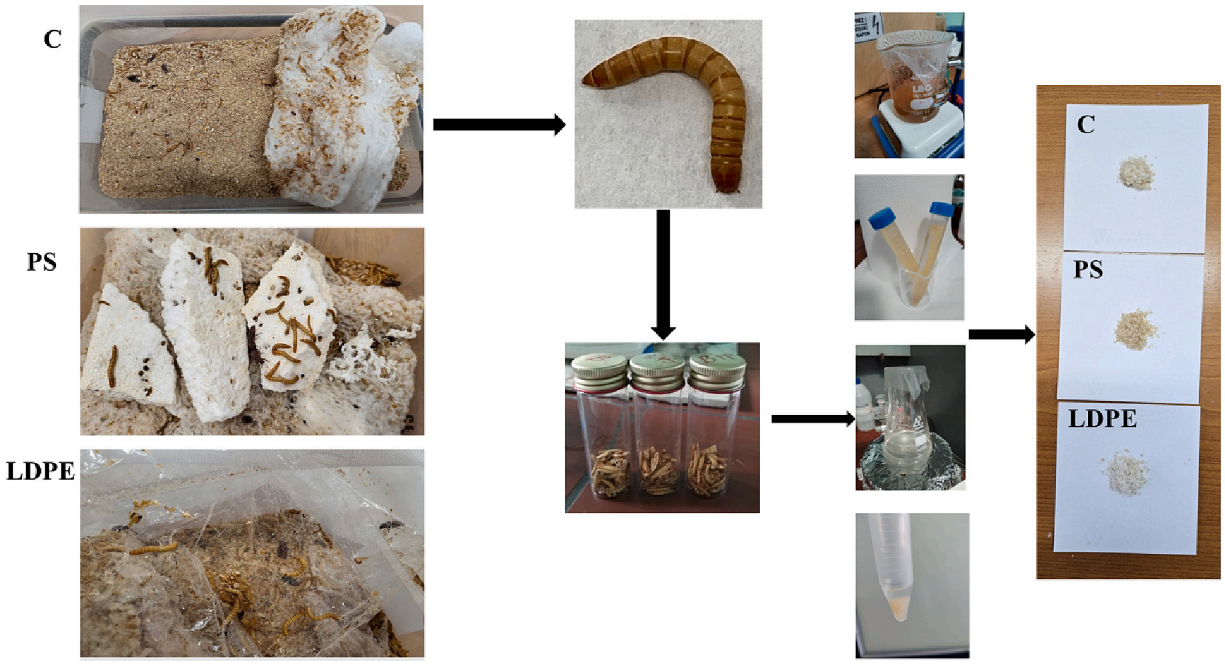

Fig. 1. Schematic illustration of extraction steps of chitin from freeze dried exoskeletons of *Tenebrio molitor* larvae fed with wheat bran (C-control group), wheat bran with added polystyrene (PS group), or plastic kitchen wrap (LDPE group).

distilled water until the pH became neutral, isolated chitin was dried in air oven at 60 °C for 24 h and weighed. The yield of obtained chitin was calculated as [36]:

$$\text{Chitin yield } (\%) = \text{weight of chitin/weight of the insect powder} \times 100 \quad (1)$$

2.3.3. ATR-FTIR spectroscopy

ATR-FTIR spectroscopy (SpectrumTwo, Perkin Elmer,Waltham, MA, USA) was used to characterize isolated chitin from exoskeletons of *T. molitor* larvae from the control group, as well as those from groups fed with PS and LDPE based plastic materials. This analysis was used to determine the presence of IR bands characteristic for α-chitin in all 3 extracted chitin samples. Transmittance values were evaluated in the range from 4000 to 400 cm^{-1}, with a resolution of 8 cm^{-1} and scan rate of 8 accumulations.

2.3.4. Field emission scanning electron microscopy (FESEM) combined with energy dispersive X-ray spectroscopy (EDS)

The morphology and elemental analysis of each isolated chitin sample was analyzed using FESEM on a FEI SCIOS 2 Dual Beam electron microscope (Thermo Fischer Scientific, Waltham MA, USA) operating at an acceleration voltage of 10 kV and combined with an Oxford Instruments EDS system. The samples were prepared for analysis by depositing the chitin flakes onto carbon tape and a thin gold layer was sputtered over them. EDS elemental analysis was performed at magnification of 500× in triplicate.

2.3.5. X-ray diffraction (XRD)

The crystallinity of extracted chitin was determined by recording X-ray diffraction patterns on a Rigaku Ultima IV diffractometer (Tokyo, Japan) in the range 2–40°, step size 0.2°, with CuK_α radiation. The crystallinity index (CrI) was calculated as [36,37]:

$$CrI\ (\%) = F_c/(F_c + F_a) \times 100 \quad (2)$$

where F_c is the area of crystalline peaks $I_{(110)}$ and $I_{(020)}$ corresponding to (110) and (020) crystalline diffraction planes of orthorhombic α-chitin at $2\theta = 19.3$ and 9.2°, respectively and F_a is the area of the amorphous peaks in the measured XRD spectrum.

2.3.6. Thermogravimetric analysis

TG/DTA analysis of obtained chitin samples from all three groups (C, PS and LDPE) was performed using a Perkin Elmer STA 6000 simultaneous TG/DTA analyzer (Waltham, MA, USA) in nitrogen atmosphere, heating rate 20°/min from room temperature to 550 °C.

2.4. Statistical analysis

Statistical analysis was performed with the Statistica software (version 6, StatSoft Poland, Krakow, Poland). Analysis of variance (ANOVA) was used to determine differences between means followed by the post hoc Fisher test and Tukey honest significance difference (HSD) test at the significance threshold of $p < 0.05$.

3. Results and discussion

3.1. ATR-FTIR spectra of feed mixtures and frass

The measured spectra of bran, polystyrene and the kitchen wrap used to feed the larvae are shown in Fig. 2a-c. In the measured spectrum for industrial bran fed to the control group (Fig. 2a) the strong wide band centered at ≈3288 cm^{-1} can be attributed to the O—H stretching vibration of hydroxyl groups [40,41], the sharp band at ≈2923 cm^{-1} can be attributed to CH stretching vibrations [40], while the smaller one at ≈2857 cm^{-1} can be attributed to CH_2 stretching vibration [42,43]. The band at ≈1742 cm^{-1} can be attributed to C═O stretching vibrations [44], while the bands at 1638 cm^{-1} and 1410 cm^{-1} can be attributed to C═O asymmetric and symmetric stretching vibrations [41], though a band at ≈1420 cm^{-1} has also been attributed to CH_2 bending [40,42] so some overlapping is possible. The prominent peak centered at ≈1017 cm^{-1} can be attributed to C—O stretching vibrations of the pyranose ring [40]. The bands in the range below 900 cm^{-1} can be attributed to α and β glucan configurations [45], while the band at ≈874 can be attributed to the α-glycosidic bond [40].

The measured FTIR spectrum of polystyrene (PS) samples (Fig. 2b) corresponded (0.969224) to the AP0067 polystyrene spectrum in the FTIR device software. According to Bhutto et al. [46] bands in the region 3126–2976 cm^{-1} can be assigned to C—H stretching of benzene ring CH

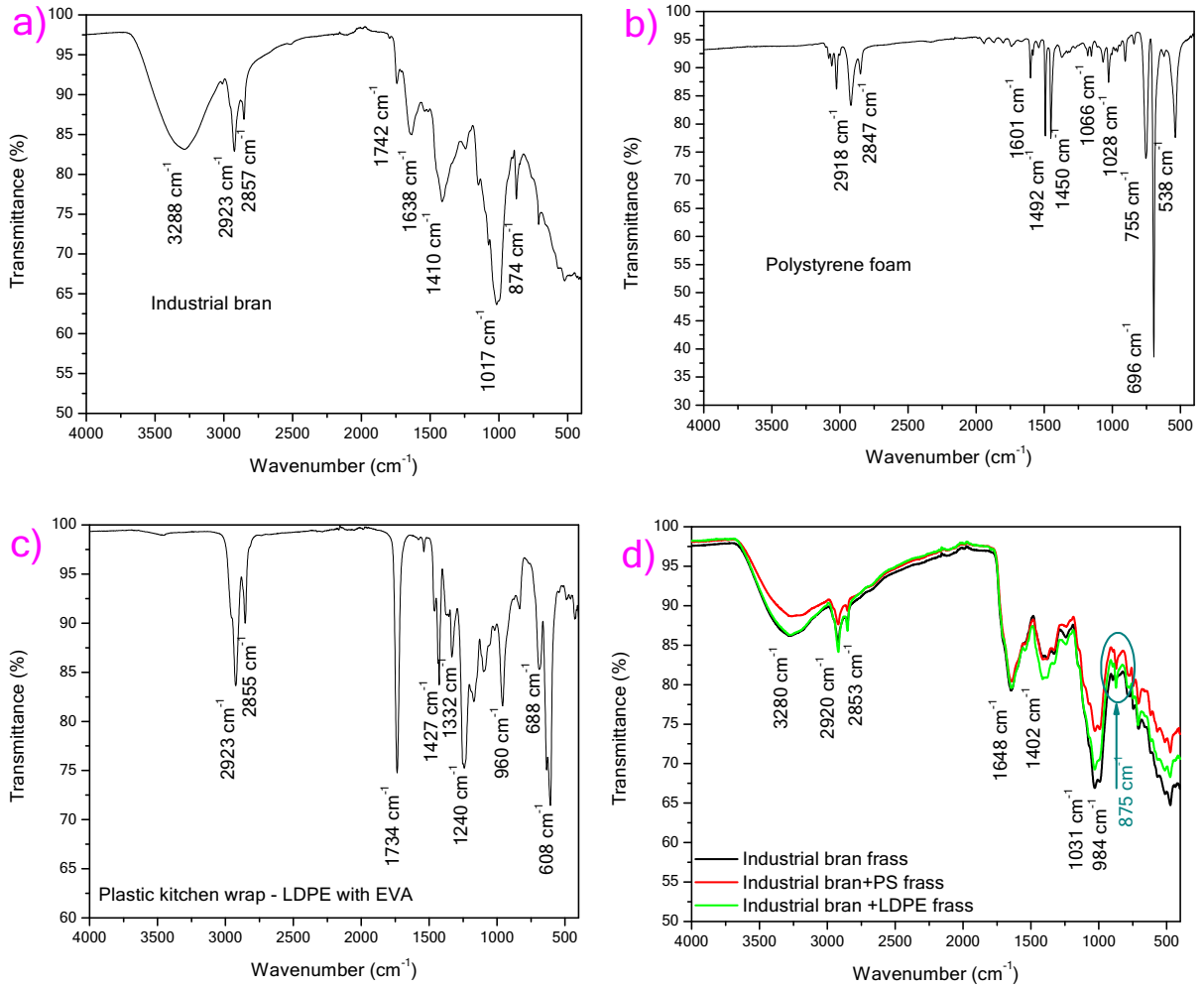

Fig. 2. FTIR spectra of industrial bran (**a**), polystyrene foam (**b**), kitchen plastic wrap containing low density polythylene (LDPE) and ethylene vinyl acetate (EVA) (**c**), and frass from *T. molitor* larvae fed with wheat bran (C-control group-black line), wheat bran with added polystyrene (PS group-red line), and plastic kitchen wrap (LDPE group-green line), green circle marks the additional band noted in the spectra of *T. molitor* fed polystyrene or plastic kitchen wrap (**d**).

groups on the PS side-chain, while bands at ≈2918 cm^{-1} and 2847 cm^{-1} are due to C—H stretching vibration of the CH_2 and CH group on the main PS chain, respectively. The bands at ≈1601 cm^{-1} and 1493 cm^{-1} can be attributed to C—C stretching frequency and C—H stretching vibrations of the ring in plane (benzene ring) [47], while the band at ≈1450 cm^{-1} is due to the C—H deformation of CH_2 [46]. The bands at ≈1066 and 1028 cm^{-1} and also ≈755 and 696 cm^{-1} can be assigned to C—H bending vibrations of the ring in plane and C—H out-of-plane bending vibrations of the benzene ring [46,47].

The measured spectrum of kitchen plastic wrap (Fig. 2c) contains bands that can be assigned to LDPE [17,48,49], but also bands that can be assigned ethyl-vinyl acetate (EVA) [50] that is commonly used for *co*-polymerization of plastic kitchen wrap to achieve better oxidation, UV and visible light resistance [51]. The two bands at ≈2923 and 2855 cm^{-1} can be assigned to CH_2 asymmetric and symmetric stretching vibrations [48] originating from both LDPE and EVA due to ethylene groups in both polymers [50]. The bands at ≈1734 cm^{-1} can be assigned to the C═O stretching vibration present in EVA [50]. The bands at ≈1427 and 1332 cm^{-1} can be assigned to the CH_2 and CH_3 bending vibrations present in LDPE [17,48]. The band at ≈1240 cm^{-1} can be attributed to C—O stretching vibrations, while the band at ≈960 cm^{-1} to C—H bending vibrations present in EVA [50]. The bands in the region below 900 cm^{-1} can be attributed to CH_2 rocking modes present in LDPE [48].

FTIR spectra of frass from all three groups exhibited similar bands (Fig. 2d) show a wide peak centered at ≈3280 cm^{-1} originating from O—H stretching vibration of hydroxyl groups [21,22], sharp band at ≈2920 cm^{-1} attributed to CH_2 stretching vibration, while the smaller one at ≈2853 cm^{-1} can be attributed to CH_3 stretching vibration [43,52]. The wide band at 1648 cm^{-1} can be attributed to C═O asymmetric stretching vibration, while the smaller bands in the 1482–1277 cm^{-1} region can be attributed to C═O symmetric stretching and CH_2 bending [40,41,43], though Wang et al. [52] attributed a band in this region noted in PS frass to O—H bending. The prominent 1182–917 cm^{-1} region with a peak centered at ≈1031 cm^{-1} can be attributed to C—O stretching vibrations of the carbonyl group [20]. There is also a small but sharp peak at ≈875 cm^{-1} that can be seen in the frass spectra of both PS and LDPE groups and not in the measured spectrum of the control group reared only on industrial bran. It can be assigned to C—O bending and was noted before for PS and PS + bran fed *T. molitor* larvae and confirms biodegradation of PS and LDPE plastics fed to the larvae [21,22,35]. Lou et al. [35] noted that frass from mealworms fed plastics or a co-diet of plastic + bran exhibited similar curves for both types of ingested plastic (PS and polyethylene (PE)), suggesting that the biodegradation process of plastics in the mealworm gut is comparable despite the presence of additional bran in the diet.

3.2. ATR-FTIR spectra of T. molitor exoskeletons and extracted chitin samples

FTIR spectra of freeze dried exoskeletons of *T. molitor* larvae fed with wheat bran (C-control group), wheat bran with added polystyrene (PS group), and plastic kitchen wrap (LDPE group) are shown in Fig. 3a, exhibiting the same bands that originate from chitin, proteins and lipids present in the larva exoskeleton [34,53], with no additional bands deriving from either polystyrene or the kitchen foil wrap. Thus, the amide A band due to N—H vibration of chitin acetamide can be noted ≈3279 cm^{-1} [53], while the bands at ≈2919 and 2853 cm^{-1} can be attributed to CH_2 symmetrical and CH_3 asymmetrical stretching vibrations also present in chitin [28,52]. Vibrations in the amide I and II regions are noted at ≈1631 and 1530 cm^{-1} and can be attributed to both amide bands in proteins and the polysaccharide chitin chain present in the exoskeleton [34,53]. The two smaller bands noted at ≈1455 and 1392 cm^{-1} can be attributed to CH_2 and CH_3 stretching vibrations of lipids [53]. The amide III region associated with a C═O bond is noted at ≈1237 cm^{-1}, while the bands at ≈1154, 1072 and 1058 cm^{-1} can be assigned to symmetrical C-O-C stretching and C—O stretching of the pyranose ring [34,53].

The FTIR spectra of extracted chitin were very similar for the three experimental groups confirming that the plastic present in the feed did not influence the extracted chitin (Fig. 3b). All bands recorded in the FTIR spectra for chitin, extracted from the control group and the PS and LDPE groups, correlate to α-chitin vibrations, as noted before for chitin extracted from insects [28,54]. The distinguishing feature of α-chitin are two absorptions in the amide I region of 1660–1622 cm^{-1} that are associated with two types of amides [55]. The first vibration band noted here at ≈1653 cm^{-1} is assigned to hydrogen bonding of part of the carbonyl groups inside the same chain, while the second vibration noted here at 1622 cm^{-1} is associated with the remaining carbonyl groups producing the same bond, but also an additional bond with the $–CH_2OH$ group [55]. All three recorded spectra have a band at ≈3434 cm^{-1} associated with OH (hydroxyl) stretching vibrations [39], while the bands at 3258 and 3100 cm^{-1} can be assigned to NH stretching vibrations, more precisely to NH amide vibrational bands and NH groups intramolecularly linked by H, also characteristic for α-chitin, respectively [55]. The C—H stretching (CH_3 vibration) band is noted at ≈2879 cm^{-1} and this band is generally more expressed in mealworm chitin, compared to shrimp derived chitin [39,56]. At ≈1557, 1375 and 1311 cm^{-1} we can note C═O stretching of amide II, C—H and C—N vibrations of amide III, respectively [28,55,56]. The small band at ≈1418 cm^{-1} is assigned to CH_2 vibrations and is also characteristic for α-chitin, as it is shifted to higher wavenumbers for β-chitin (commonly ≈1430 cm^{-1}) [39,57]. The C-O-C ring vibrations can be noted at ≈1155 cm^{-1} and the C—O stretching vibration region in the range 1100–1000 cm^{-1} present in chitin [34]. Below 1000 cm^{-1} we can note CH_3, CH_2, NH (amide *V*), C—O and C—C vibrations also associated with α-chitin [55].

The degree of deacetylation (*DA*) of chitin can be estimated from the measured FTIR spectra as [36,58]:

$$DA = A_{1320}/A_{1420} \times 100 \quad (3)$$

where: A_{1320} and A_{1420} are absorbance values at wavelengths of 1320 and 1420 cm^{-1}, respectively. The determined values, given in Table 1, for the three analyzed chitin samples were similar and around 98 %, and found to be in accordance with the values previously obtained for chitin extracted from *T. molitor* larvae and adults [36].

3.3. Yield, morphology and chemical composition of the extracted chitin

3.3.1. Chitin extraction yield

The yield of extracted chitin is shown in Table 1. It varied depending on what the *T. molitor* larvae were fed and was the highest for the control group (6.78 %) and the lowest for the LDPE fed group (5.29 %). If we observe the mass of dry exoskeletons we can note that the larvae fed bran with PS or LDPE were heavier and fatter than the larvae fed only with bran, but the chitin yield was lower. The obtained yields were similar to the values determined by Chalghaf et al. [36] from dried *T. molitor* larvae insect powder (deproteinization followed by demineralization - 5.3 %; demineralization followed by deproteinization - 6 %) and slightly higher than the value of 4.92 % obtained by Song et al. [58] from the whole larva body or 4.72 % obtained by Son et al. [39] from dried mealworm powder. The highest yields so far of 13.25 % were obtained by Machado et al. [59] from cuticular exoskeletons of *T. molitor* larvae. Chitin extraction yields have varied according to the stage of insect development and have been linked to the fat content, with the percentage of lipids influencing the chitin content and decreasing the yield [60,61]. This is the case here, where the fatter insects fed on a combination of bran and plastics (PS or LDPE) gave a slightly lower chitin yield, though still comparable with yields obtained for *T. molitor* dried powder showing them to be a viable source of chitin.

3.3.2. Chitin morphology and elemental analysis

Polysaccharide chitin is the primary structural component of insect and arthropod exoskeletons. In the cuticles of insects and other anthropods chitin self-assembles into 20 nm chitin nanofibers representing the foundation for all higher order chitin structures [62]. A lamellar structure is specific for α-chitin due to the arrangement and cross-linking of the chitin polymers [39]. The surface morphology of

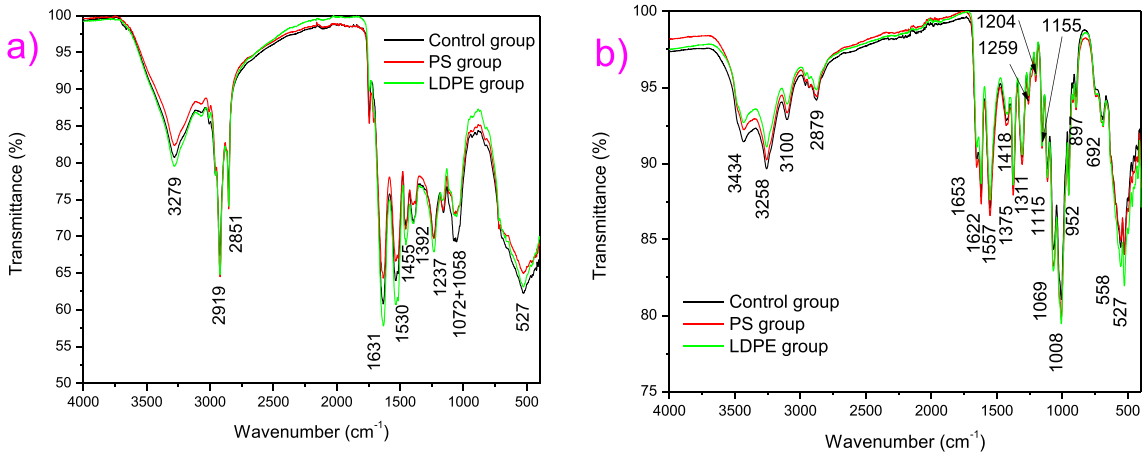

Fig. 3. FTIR spectra of freeze dried exoskeletons (**a**) and extracted chitin (**b**) of *T. molitor* larvae fed with industrial wheat bran (C-control group), wheat bran with added polystyrene (PS group), and plastic kitchen wrap (LDPE group).

Table 1
Number of exoskeletons used in the chemical extractions (*NE*), their mass after freeze drying (*ME*), mass of extracted chitin powder (*CM*), yield of extracted chitin, deacetylation degree (*DA*) determined from measured FTIR spectra using Eq. (3), elemental content of carbon (C), nitrogen (N) and oxygen (O) determined from EDS.

Group	NE	ME (g)	CM (mg)	Yield (%)	DA (%)	Elemental composition		
						C	N	O
Control	73	0.562	38.1	6.78	98.17 ± 0.33	44.77 ± 0.79	0	55.23 ± 0.79
PS	70	0.981	57.0	5.81	98.51 ± 0.02	47.96 ± 3.83	0.80 ± 1.39	51.23 ± 4.78
LDPE	70	1.187	62.8	5.29	98.61 ± 0.29	43.21 ± 1.70	2.55 ± 1.67	54.24 ± 0.39

Values are given as mean ± standard deviation, no significant differences were noted ($p < 0.05$) by Tukey's test.

insect chitin depends on the organism it originates from, its development stage and the applied extraction method [54]. Different morphologies have been noted and the extracted chitin surface can be both smooth and rough. It can be composed of nanofibers only, or combined with nanopores or pores [54]. The FESEM images (Fig. 4) showed a very similar surface morphology of chitin isolated from the control, PS and LDPE groups. Obviously, the biodegradation of polystyrene or kitchen foil wrap containing mostly LDPE does not influence the structure of chitin in *T. molitor* larvae. Low magnification (80× and 500×) images showed a lamellar, dense, and slightly rough fibrillar surface, similar to chitin obtained from *T. molitor* dried powder or commercial α-chitin obtained from shrimp [39], or other insect and crustacean sources [54,59]. Higher magnification (3500× and 10,000×) revealed a morphology containing nanofibers, multiple evenly distributed small nanopores and some intermittent larger pores with a diameter of ≈ 5 μm. This porous morphology is similar to the morphology noted by Soon et al. [63] for chitin sourced from *Zophobas morio* larvae. The chitin morphology influences application of this biopolymer, where porous morphologies are better suited for adsorption of metallic ions, fibrillar structures for tissue engineering or wound dressing and nanofiber and nanopore forms for food industry, textiles or other medical applications [54,59].

Elemental analysis of the extracted chitin samples from all three experimental groups, was also very similar, with all three samples containing carbon and oxygen, while nitrogen was present in the PS and LDPE groups and below the detection limit for the control group. The nitrogen content in chitin is an indicator of chitin purity, with 6.89 % determined in pure acetylated chitin [54]. If this value is higher protein residues are most probably present, while lower values indicate the presence of residual inorganic elements [36,54], though some authors associate a lower N content also with a low protein amount remaining in chitin [63]. This is probably the case for our samples, with the LDPE group showing the highest nitrogen content (2.55 %) and lowest amount of residual inorganic elements. Many parameters can affect the chemical composition of chitin and they include the applied extraction procedure, order of extraction steps (whether demineralization or deproteinization was first), and also the extraction time and temperature [36,63]. Fine tuning of these parameters can give chitin with properties closer to the ideal values.

3.4. Chitin crystalline properties

XRD analysis was performed to determine the crystallinity of chitin isolated from freeze dried exoskeletons of *T. molitor* larvae from all three experimental groups, and the obtained XRD diffractions are presented in Fig. 5. The spectra were very similar for all chitin obtained from *T. molitor* exoskeleton larvae fed only bran, or bran combined with polystyrene (PS group) or kitchen plastic wrap (LDPE group). Two sharp peaks characteristic for α-chitin at ≈ 9.2 and 19.2° can be observed, corresponding to the (020) and (110) diffraction planes of the α-chitin

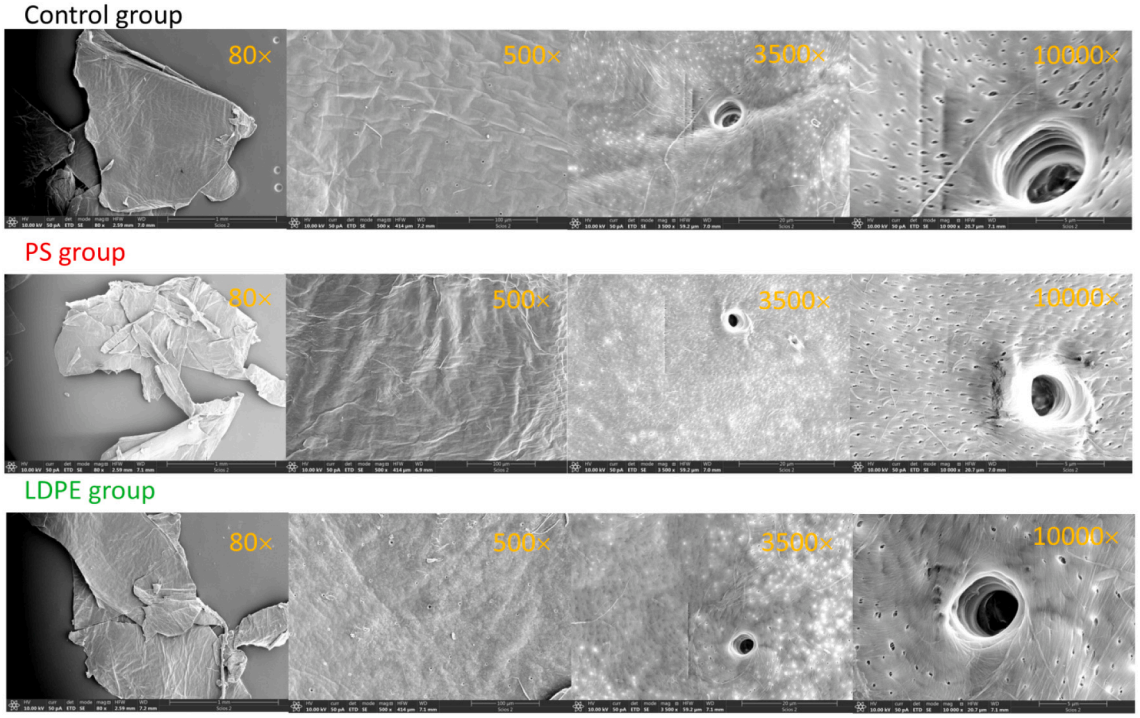

Fig. 4. FESEM images of chitin samples extracted from *T. molitor* larvae from control, PS and LDPE groups, given in different magnifications (80, 500, 3500 and 10,000 ×).

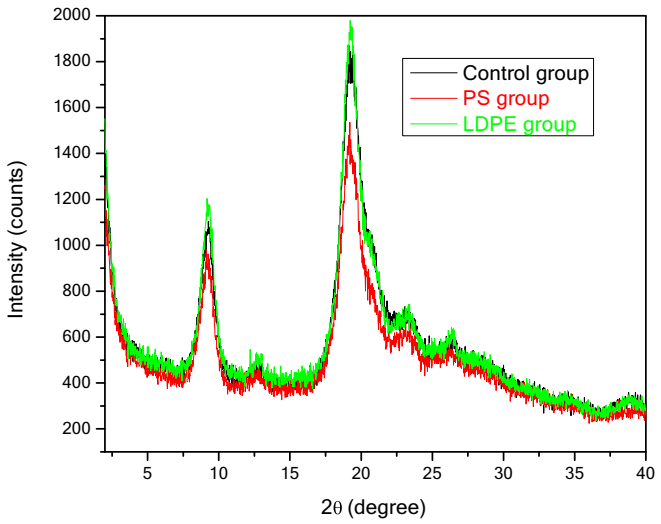

Fig. 5. X-ray diffraction spectra of chitin extracted from *T. molitor* control, PS and LDPE groups.

orthorhombic crystalline structure [55,59]. This type of chitin is found in rigid structures, such as insect or crustacean exoskeletons. The other smaller peaks (as shown in Table 2) can also be attributed to α-chitin and their values are within the range determined for α-chitin extracted from *T. molitor* larvae and adults, different insects and shrimp [39,54,59,64]. Dense packing of polysaccharide chains is a characteristic of α-chitin and it is due to antiparallel arrangement of polymeric chains [59].

The crystallinity index (CrI) was calculated using Eq. (2). The obtained values are given in Table 2, and are in the range of values previously determined for chitin obtained from *T. molitor* larvae and adults, other insects and shrimp shells [39,54]. This parameter is quite significant when evaluating the potential application of the extracted chitin, and it is influenced by the applied extraction method as well as the source organism [59]. Mohan et al. [54] showed that for insects the CrI can vary between 33 and 96.4 %, though chitin CrI is mainly in the range 60–90 %. Chitin with a higher CrI is more suited for cosmetic and biomedical applications, while lower CrI is more suited for removing contaminants (such as heavy metals or polluting dyes) [54,59,64]. In our case we obtained CrI between 66.5 and 62 %, with CrI the lowest for the LDPE group, and highest for the control group that was overall higher than 57.85 % determined by Son et al. [39] and comparable to 67.8 and 64.1 % determined by Hajji et al. [37] for crab and shrimp chitins. Future work will focus on identifying possible application fields taking into account the crystallinity and morphology.

Another parameter that can be calculated from the measured XRD spectra is the crystallite size (D) using the Scherer equation:

$$D = k \cdot \lambda / (\beta \cdot cos\theta) \quad (4)$$

where k is 0.9, λ is the measuring wavelength (0.154178), β is the width of half-height of the analyzed peak and θ is the diffraction angle of the analyzed peak. We used the highest intensity peak at 19.3, diffraction plane (110) and obtained 4 nm for the control group and 5 nm for the PS and LDPE groups (Table 2). These values are comparable with the crystallite size determined by Triunfo et al. [64] for chitin obtained from various developmental stages of *Hermetia illucens* (4–6 nm) and commercial shrimp chitin sample (6 nm).

3.5. Thermogravimetric analysis of chitin samples

Fig. 6 shows TG and DTG curves measured for the chitins extracted from freeze dried exoskeletons of *T. molitor* larvae fed with wheat bran (C-control group), wheat bran with added polystyrene (PS group), and plastic kitchen wrap (LDPE group). The first temperature intervals of weight loss (30–110 °C) with approximately 7 % (*w*/w) for control group, 4 % (w/w) for PS, and 5 % (w/w) for the LDPE group could be attributed to evaporation of water that was physically and chemically adsorbed in the obtained chitin [65]. The second weight losses, occurring in the range 120–410 °C, were 70 % (w/w), 62 % (w/w) and 70 % (w/w) of the initial weight of chitin, and were due to the decomposition of the acetylated and deacetylated units of the chitin chain [66]. After the maximum heating temperature (550 °C), the percentage of residual mass was 17 %, 13 % and 3 % (w/w) for chitin samples from the control, PS and LDPE groups, respectively. These values are within the range of values determined previously for chitin extracted from *T. molitor* larvae and other insects and can be linked to impurities originating from not completely removed minerals [59]. The residual mass was the lowest for chitin extracted from *T. molitor* fed plastic kitchen wrap and bran, indicating the lowest remaining mineral content. The temperature at which the maximum degradation of α-chitin occurred (DTG_{max}) was 383C for the chitin extracted from the residues of freeze dried exoskeletons of *T. molitor* larvae fed with wheat bran, 356C for the chitin extracted from the residues of freeze dried exoskeletons of *T. molitor* larvae fed with wheat bran wheat bran with added polystyrene (PS group) and 354C for the chitin extracted from the residues of freeze dried exoskeletons of *T. molitor* larvae fed with wheat bran wheat bran with added plastic kitchen wrap. The chitin samples sourced from *T. molitor* exoskeleton fed a mixture of plastic (PS or LDPE) and bran had a similar and slightly lower DTG_{max} value, but all obtained values are in agreement with previously obtained results where the DTG_{max} value of α-chitin sourced from insects was determined to be above 350 °C and generally showed two mass loss steps [54,65,67].

4. Conclusion

Chitin samples were obtained from *T. molitor* exoskeleton from larvae fed plastic (polystyrene -PS or kitchen plastic wrap – mainly LDPE) and bran and only bran (control group). The chitin yield, structure, morphology, crystallinity index, deacetylation degree and thermal degradation properties determined by XRD, ATR-FTIR, FESEM, EDS and TG/DTA analysis were similar and comparable to other insect sources and conventional sources such as shrimp or crab shells. ATR-FTIR spectra of the insect frass confirmed biodegradation of the consumed plastic, while exoskeleton spectra of all three larvae groups were comparable and contained no residual plastic. This preliminary study shows the potential of utilization of insects fed plastic as sources of chitin. This enables further studies into potential use of insects and their residues from plastic biodegrading insect farms as chitin sources and further development and optimization of the extraction procedure.

Table 2
Diffraction peaks for chitin samples determined from measured XRD spectra, crystallinity index (*CrI*) determined using Eq. (2) and crystallite size (*D*) determined using the Scherer Eq. (4).

Group	Diffraction peaks (2θ, °)							CrI (%)	D (nm)
Control	9.2	12.8	19.2	23.3	26.4	27.8	39.2	66.5	4
PS	9.2	12.2	19.2	23.4	26.3	28.6	38.7	65.8	5
LDPE	9.1	12.4	19.2	23.1	26.1	28.9	39.3	62.0	5

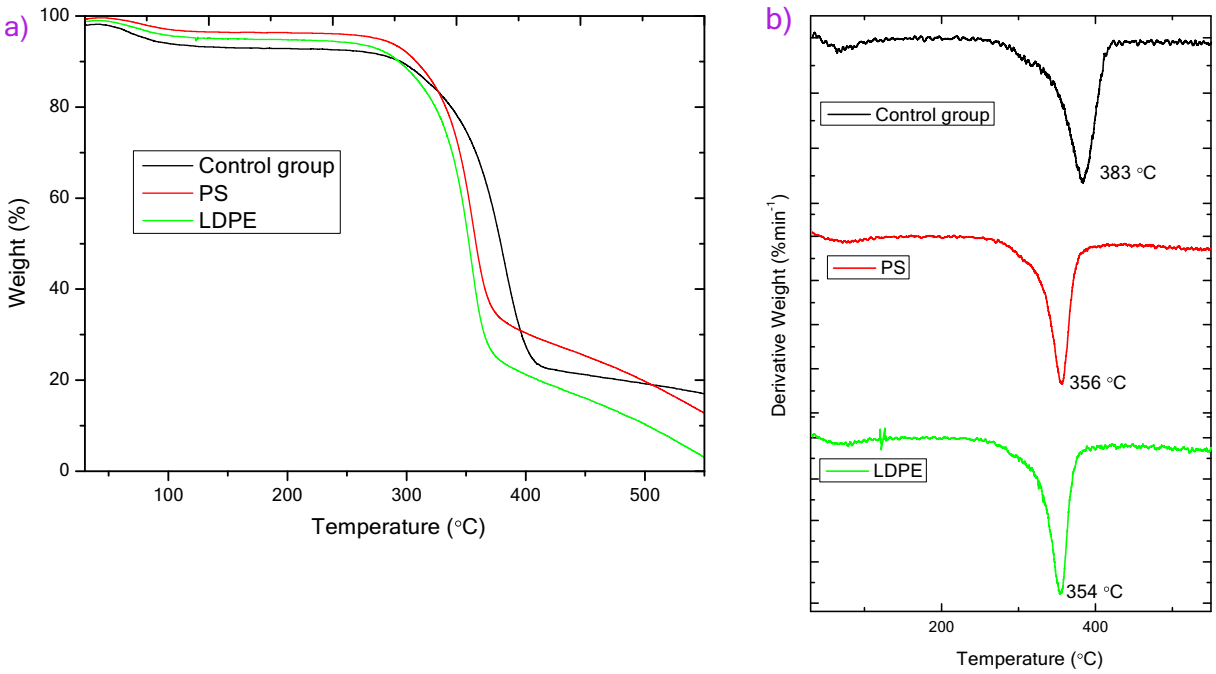

Fig. 6. TG (a) and DTG (b) curves obtained for chitin extracted from *T. molitor* control, PS and LDPE groups.

Ethics approval

All animal procedures were in compliance with Directive 2010/63/EU on the protection of animals used for experimental and other scientific purposes and were approved by the Ethical Committee for the Use of Laboratory Animals of the Institute for Biological Research "Siniša Stanković," National Institute of the Republic of Serbia, University of Belgrade.

CRediT authorship contribution statement

Larisa Ilijin: Writing – original draft, Visualization, Investigation, Conceptualization, Methodology. **Maria Vesna Nikolić:** Writing – original draft, Visualization, Methodology, Investigation, Formal analysis, Conceptualization. **Zorka Z. Vasiljević:** Writing – review & editing, Investigation, Formal analysis. **Dajana Todorović:** Writing – review & editing, Investigation. **Marija Mrdaković:** Validation, Writing – review & editing. **Milena Vlahović:** Supervision, Methodology, Conceptualization. **Dragana Matić:** Writing – review & editing, Methodology. **Nenad B. Tadić:** Investigation, Writing – review & editing. **Vesna Perić-Mataruga:** Writing – review & editing, Project administration, Funding acquisition.

Declaration of competing interest

The authors declare that they have no known competing financial interests or personal relationships that could have appeared to influence the work reported in this paper.

Data availability

Data will be made available on request.

Acknowledgements

We would like to express our gratitude to Dr. Vladimir Rajić (Vinca National Institute) for FESEM and EDS measurements and Prof. Goran Grubić for statistical analysis. This work was funded by the Ministry for Science, Technological Development and Innovations of the Republic of Serbia, contracts 451-03-66/2024-03/200053 (M.V.N. and Z.Z.V.) and 451-03-47/2023-1//200007 (L.I., D. T., M.M., M.V., D. M. and V. P. M.).

References

[1] N. Alexandratos, J. Bruinsma, World agriculture towards 2030/2050: the 2012 revision, in: ESA Working Paper No. 12-03, FAO, Rome, 2012. https://www.fao.org/3/ap106e/ap106e.pdf.
[2] A. van Huis, J. Van Herbeeck, H. Klunder, E. Mertens, A. Halloran, G. Muir, P. Vantomme, Edible insects - future prospects for food and feed security, in: FAO Forestry Paper 171, FAO and Wageningen UR, Food and Agriculture Organization of the United Nations, 2013. https://www.fao.org/3/i3253e/i3253e.pdf.
[3] J.I. Blakstad, R. Strimbeck, J. Poveda, A.M. Bones, R. Kissen, Frass from yellow mealworm (*Tenebrio molitor*) as plant fertilizer and defense priming agent, Biocatal. Agric. Biotechnol. 53 (2023) 102862, https://doi.org/10.1016/j.bcab.2023.102862.
[4] F.G. Horgan, D. Floyd, E.A. Mundaca, E. Crisol-Martínez, Spent coffee grounds applied as a top-dressing or incorporated into the soil can improve plant growth while reducing slug herbivory, Agriculture 13 (2023) 257, https://doi.org/10.3390/agriculture1302025.
[5] D.J.C. Hutabarat, D. Mangindaan, Cultivation of black soldier Fly (*Hermetia illucens*) larvae for the valorization of spent coffee ground: a systematic review and bibliometric study, Agriculture 14 (2024) 205, https://doi.org/10.3390/agriculture14020205.
[6] L.S. Queiroz, N.F.N. Silva, F. Jessen, M.A. Mohammadifar, R. Stephani, A.F. de Carvalho, I.T. Perrone, F. Casanova, Edible insect as an alternative protein source: a review on the chemistry and functionalities of proteins under different processing methods, Heliyon 9 (2023) e14831, https://doi.org/10.1016/j.heliyon.2023.e14831.
[7] J.C. Ribeiro, M.E. Pintado, L.M. Cunha, Consumption of edible insect and insect based foods: a systematic review of sensory properties and evoked emotional response, Compr. Rev. Food Sci. Food Saf. 23 (2024) 1–45, https://doi.org/10.1111/1541-4337.13247.
[8] R. Moruzzo, F. Riccioli, S.E. Diaz, C. Secci, G. Poli, S. Mancini, Mealworm (*Tenebrio molitor*): potential and challenges to promote circular economy, Animals 11 (2021) 2568, https://doi.org/10.3390/ani11092568.
[9] V. Kotsou, T. Chatzimitakos, V. Athanasiadis, E. Bozinou, C.G. Athanassiou, S. I. Zalas, Innovative applications of *Tenebrio molitor* larvae in food product development: A comprehensive review, Food 12 (2023) 4223, https://doi.org/10.3390/foods12234223.
[10] J. Hong, T. Han, Y.Y. Kim, Mealworm (*Tenebrio molitor* larvae) as an alternative protein source for monogastric animal: a review, Animals 10 (2020) 2068, https://doi.org/10.3390/ani10112068.
[11] L. Syahrulawal, M. Torske, R. Sapkota, G. Naess, P. Khanil, Improving the nutritional values of yellow mealworm *Tenebrio molitor* (Coleoptera: Tenebrionidea) larvae as an animal feed ingredient: a review, J. Anim. Sci. Biotechnol. 14 (2023) 146, https://doi.org/10.1186/s40104-023-00945-x.
[12] S. Errico, A. Spagnoletta, A. Verardi, S. Moliteni, S. Dimatteo, P. Sangiorgio, *Tenebrio molitor* as a source of interesting natural compounds, their recovery

process, biological effects and safety aspects, Compr. Rev. Food Sci. Food Saf. 21 (2022) 148–197, https://doi.org/10.1111/1541-4337.12863.
[13] A. Gkinali, A. Matsakidou, E. Vasilieou, A. Paraskevopolou, Potentiality of *Tenebrio molitor* larva-based ingredients for the food industry: a review, Trends Food Sci. Technol. 119 (2022) 495–509, https://doi.org/10.1016/j.tifs.2021.11.024.
[14] K. Kik, B. Bukowska, P. Sicinska, Polystyrene nanoparticles: sources, occurrence in the environment, distribution in tissues, accumulation and toxicity to various organisms, Environ. Pollut. 262 (2020) 114297, https://doi.org/10.1016/j.envpol.2020.114297.
[15] A. Turner, Foamed polystyrene in the marine environment: sources, additives, transport, behavior and impacts, Environ. Sci. Technol. 54 (2020) 10411–10420, https://doi.org/10.1021/acs.est.0c03221.
[16] A. Ergut, Y.A. Levendis, J. Carlson, Emissions from the combustion of polystyrene, styrene and ethylbenzene under diverse conditions, Fuel 86 (2007) 1789–1799, https://doi.org/10.1016/j.fuel.2007.01.009.
[17] Z. Montazer, M.B. Habibi-Najafi, M. Mohebdi, A. Oromiehei, Microbial degradation of UV-penetrated low-density polyethylene films by novel polyethylene-degrading bacteria isolated from plastic dump soil, J. Polym. Environ. 26 (2018) 3613–3625, https://doi.org/10.1007/s10924-018-1245-0.
[18] A.C. Vivekanand, S. Mohapatra, V.K. Tyagi, Microplastics in aquatic environment: challenges and perspectives, Chemosphere 282 (2021) 131151, https://doi.org/10.1016/j.chemosphere.2021.131151.
[19] P. Mishra, P. Charda, P. Kumar, R. Pandit, M. Joshi, M. Kumar, C. Joshi, Exploring genetic landscape of low-density polyethylene degradation for sustainable troubleshooting of plastic pollution at landfills, Sci. Total Environ. 912 (2024) 168882, https://doi.org/10.1016/j.scitotenv.2023.168882.
[20] S.S. Yang, A.M. Brandon, J.C.A. Flanagan, J. Yang, D. Ning, S.Y. Cai, H.Q. Fan, Z. Y. Wang, J. Ren, E. Benbow, N.Q. Ren, R.M. Waymouth, J. Zhou, C.S. Criddle, W. M. Wu, Biodegradation of polystyrene wastes in yellow mealworms (larvae of *Tenebrio molitor* Linneaus): factors affecting biodegradation rates and the ability of polystyrene fed larvae to complete their life cycle, Chemosphere 191 (2018) 979–989, https://doi.org/10.1016/j.chemosphere.2017.10.117.
[21] S.S. Yang, W.M. Wu, A.M. Brandon, H.Q. Fan, J.P. Receveur, Y. Li, Z.Y. Wang, R. Fan, R.L. McClellan, S.H. Gao, D. Ning, D.H. Philips, B.Y. Peng, H. Wang, S. Y. Cai, P. Li, W.W. Cai, L.Y. Ding, J. Yang, M. Zheng, C.S. Criddle, Ubiquity of polystyrene digestion and biodegradation within yellow mealworms, larvae of *Tenebrio molitor* Linnaeus (Coleoptera: Tenebrionidae), Chemosphere 212 (2018) 262–271, https://doi.org/10.1016/j.chemosphere.2018.08.078.
[22] L. Yang, J. Gao, Y. Liu, G. Zhuang, X. Peng, W.M. Wu, X. Zhuang, Biodegradation of expanded polystyrene and low-density polyethylene foams in larvae of *Tenebrio molitor* Linnaeus (Coleoptera: Tenebrionidae): broad versus limited extent depolymerization and microbe-dependence versus independence, Chemosphere 262 (2021) 127818, https://doi.org/10.1016/j.chemosphere.2021.127818.
[23] K. ur Rehman, C. Hollah, K. Wietsotzki, V. Heinz, K. Aganovic, R. ur Rehman, J. I. Petrusan, L. Zheng, J. Zhang, S. Sohail, M. K. Mansoor, C. I. Rumbos, C. Athassiou, M. Cai, Insect-derived chitin and chitosan: a still unexploited resource for the edible insect sector, Sustainability 15 (2023) 4864 https://doi.org/10.3390/su15064864.
[24] S. Muthukrishnan, Y. Arakane, M.Y. Noh, S. Mun, H. Merzendorfer, C. Boehringer, B. Wellmeyer, Q. Yang, M. Qu, L. Liu, Chapter one - chitin in insect cuticle, in: M. Sugumaran (Ed.), Advances in Insect Physiology 62, Academic Press, 2022, pp. 1–110, https://doi.org/10.1016/bs.aiip.2022.03.001.
[25] H. Merzendorfer, L. Zimoch, Chitin metabolism in insects: structure, function and regulation of chitin synthases and chitinases, J. Exp. Biol. 206 (2003) 4393–4412, https://doi.org/10.1242/jeb.00709.
[26] D. Doucet, A. Retnakaran, Chapter six - insect chitin: metabolism, genomics and Pest management, in: Tarlochan S. Dhadialla (Ed.), Advances in Insect Physiology 43, Academic Press, 2012, pp. 437–511, https://doi.org/10.1016/B978-0-12-391500-9.00006-1.
[27] T. Ganz, Lysozyme, in: G.J. Laurent, S.D. Shapiro (Eds.), Encyclopedia of Respiratory Medicine, Academic Press, 2006, pp. 649–653, https://doi.org/10.1016/B0-12-370879-6/00228-3.
[28] N. Khatami, P. Guerrero, P. Martin, E. Quintela, V. Ramos, L. Sao, A.L. Cortajarena, K. de la Caba, S. Camarero-Espinosa, A. Abarrategi, Valorization of biological waste from insect-based food industry: assessment of chitin and chitosan potential, Carbohydr. Polym. 324 (2024) 121529, https://doi.org/10.1016/j.carbpol.2023.121529.
[29] H. El Knidri, J. Dahmani, A. Addaou, A. Laajeb, A. Lahsini, Rapid and efficient extraction of chitin and chitosan for scale-up production: effect of process parameters on deacetylation degree and molecular weight, Int. J. Biol. Macromol. 139 (2019) 1092–1102, https://doi.org/10.1016/j.ijbiomac.2019.08.079.
[30] S. Kumari, R. Kishor, Chapter 1 - chitin and chitosan: origin, properties, and applications, in: S. Gopi, S. Thomas, A. Pius (Eds.), Handbook of Chitin and Chitosan, Elsevier, 2020, pp. 1–33, https://doi.org/10.1016/B978-0-12-817970-3.00001-8.
[31] P. Baharlouei, A., Rahman chitin and chitosan: prospective biomedical applications in drug delivery, cancer treatment, and wound healing, Mar. Drugs 20 (2022) 460, https://doi.org/10.3390/md20070460.
[32] X. Yang, J. Liu, Y. Pei, X. Zheng, K. Tang, Recent progress in preparation and application of nano-chitin materials, Energy Environ. Mater. 3 (2020) 492–515, https://doi.org/10.1002/eem2.12079.
[33] T. Jozwiak, U. Filipkowska, T. Bakula, B. Bralewska-Piotrawicz, K. Karczmaiczyk, M. Gierziewska, E. Olewnik-Kruuszkowska, N. Szyrynska, B. Lewczuk, The use of chitin from the molts of mealworm (*Tenebrio molitor*) for the removal of anionic and cationic dyes from aqueous solutions, Materials 16 (2023) 545, https://doi.org/10.3390/ma16020545.
[34] E. Pasquier, M. Beaumont, B.D. Mattos, C.G. Otoni, A. Winter, T. Rosenau, M. N. Belgacem, O.J. Royas, J. Bras, Upcycling byproducts from insect (fly larvae and mealworm) farming into chitin nanofibers and films, ACS Sust. Chem. Eng. 9 (2021) 13618–13629, 10.1021.acssuschemeng.1c05035.
[35] Y. Lou, Y. Li, B. Lu, Q. Liu, S.S. Yang, B. Liu, N. Ren, W.M. Wu, D. Xing, Response of the yellow mealworm (*Tenebrio molitor*) gut microbiome to diet shifts during polystyrene and polyethylene degradation, J. Hazard. Mater. 416 (2021) 126222, https://doi.org/10.1016/j.jhazmat.2021.126222.
[36] M. Chalghaf, K. Charradi, R. Ksouri, Q.A. Alsulami, A. Jaouani, S.M.A.S. Keshk, El A. Hayouni, Physicochemical characterization of chitin extracted by different treatment sequences from edible insect, Int. J. Biol. Macromol. 253 (2023) 127156, https://doi.org/10.1016/j.ijbiomac.2023.127156.
[37] S. Hajji, I. Younos, O. Ghorbel-Bellcaj, R. Hajji, M. Rinaudo, M. Nasri, K. Jellouli, Structural differences between chitin and chitosan extracted from three different marine sources, Int. J. Biol. Macromol. 65 (2014) 298–306, https://doi.org/10.1016/j.ijbiomac.2014.01.045.
[38] C.S. Shin, D.Y. Kim, W.S. Shin, Characterization of chitosan extracted from mealworm beatle (*Tenebrio molitor, Zophobas morio*) and Rhinoceros beetle (*Allomyrina dichotoma*) and their antibacterial activities, Int. J. Biol. Macromol. 125 (2019) 72–77, https://doi.org/10.1016/j.ijbiomac.2018.11.242.
[39] Y. J. Son, I. K. Hwang, C. W. Nho, S. M. Kim, S. H. Kim, Determination of carbohydrate composition in mealworm (*Tenebrio molitor* L.) larvae and characterization of mealworm chitin and chitosan, Foods 10 (2021) 640 https://doi.org/10.3390/foods10030640.
[40] X.L. Shang, C.Y. Liu, H.Y. Dong, H.H. Peng, Z.Y. Zhu, Extraction, purification, structural and antioxidant activity of polysaccharides from wheat bran, J. Mol. Struct. 1233 (2021) 130096, https://doi.org/10.1016/j.molstruct.2021.130096.
[41] Q. Chen, R. Wang, Y. Wang, X. Hu, N. Liu, M. Song, Y. Yang, N. Yiu, J. Qi, Characterization and antioxidant activity of what bran polysaccharides modified by *Saccharomyces cervisiae* and *Bacillus subtilis* fermentation, J. Cereal Sci. 97 (2021) 103157, https://doi.org/10.1016/j.jcs.2020.103157.
[42] A.E. Ghaly, F.N. Alkoaik, The yellow mealworm as a novel source of protein, Am. J. Agric. Biol. Sci. 4 (2009) 319–331, https://doi.org/10.1016/j.nfs.2020.10.001.
[43] A. J. da Silva Lucas, E. D. Oreste, H. L. G. Costa, H. M. Lopez, C. D. M. Saad, C. Prentice, Extraction, physicochemical characterization and morphological properties of chitin and chitosan from cuticles of edible insects, Food Chem. 343 (2021) 128550 https://doi.org/10.1016/j.foodchem.2020.128550.
[44] T.P. Silva, A.N. Ferreira, F.S. de Alberquerque, A.C. de Almeida Barros, J.M.R. da Luz, F.S. Gomes, H.J.V. Pereira, Box-Belinken experimental design for the optimization of enzymatic saccharification of wheat bran, Biomass Convers. Biorefinery (2021), https://doi.org/10.1007/S13399-021-01378-0.
[45] Q.Q. Lv, J.J. Cao, R. Liu, H.Q. Chen, Structural characterization, α-amylase and α-glucosidase inhibitory activities of polysaccharides from wheat bran, Food Chem. 341 (2021) 128218, https://doi.org/10.1016/j.foodchem.2020.128218.
[46] A. Bhutto, D. Vesely, B.J. Gabrys, Miscibility and interactions in polystyrene and sodium sulfonated polystyrene with poly(vinyl methyl ether) PVME blends. Part II: FTIR, Polymer 44 (2003) 6627–6631, https://doi.org/10.1016/j.polymer.2003.08.005.
[47] A. Kumar, L.K. Jangir, Y. Kumari, M. Kumar, V. Kumar, K. Awasthi, Optical and structural study of polyaniline/polystyrene composite films, Micromol. Symp. 357 (2015) 229–234, https://doi.org/10.1002/masy.201500039.
[48] H. Rajandas, S. Parimannan, K. Sathasivam, M. Ravichandran, L.S. Yiu, A novel FTIR-ATR spectroscopy based technique for the estimation of low density polyethylene biodegradation, Polym. Test. 21 (2012) 1094–1099, https://doi.org/10.1016/j.polymertesting.2012.07.015.
[49] M.R. Jung, D. Horgen, S.V. Orski, V.C. Rodriguez, K.L. Beers, G.H. Balazs, T. T. Jones, T.M. Work, K.C. Brignac, S.J. Royer, K.D. Hyrenback, B.A. Jonsen, J. M. Lynch, Validation of ATR FTIR to identify polymers of plastic marine debris, including those ingested by marine organisms, Mar. Pollut. Bull. 127 (2018) 704–716, https://doi.org/10.1016/j.marpolbul.2017.12.061.
[50] S. Azizi, C.M. Oullet-Plamandon, P. Nguyen-Tri, M. Frechetto, Electrical, thermal and rheological properties of low-density polyethylene/ethylene vinyl acetat/graphene-like composite, Comp. Part B 177 (2019) 107288, https://doi.org/10.1016/j.compositesb.2019.107288.
[51] S.W. Holman, T.F. Emmett, M.D. Cole, A quantitative assessment of the chemical variation in food grade polyethylene cling films, a common wrapping material for illicit drugs, using attenuated total reflection Fourier transform infrared spectroscopy, Anal. Methods 4 (2012) 1667–1673, https://doi.org/10.1039/c2ay05889h.
[52] Y. Wang, L. Luo, X. Li, J. Wang, H. Wang, C. Chen, H. Guo, T. Han, A. Zhou, X. Zhao, Different plastics ingestion preferences and efficiencies of superworm (Zophobas atratus Fab.) and yellow mealworm (*Tenebrio molitor* Linn.) associated with distinct gut microbioma changes, Sci. Total Environ. 837 (2022) 155719 https://doi.org/10.1016/j.scitotenv.2022.155719.
[53] T. Jozwiak, U. Filipkowska, T. Bakula, The use of exoskeletons and molts of farmed mealworm (*Tenebrio molitor*) for the removal of reactive dyes from aqueous solutions, Appl. Sci. 13 (2023) 7379, https://doi.org/10.3390/app13137379.
[54] K. Mohan, A.R. Ganesan, T. Muralisankar, R. Jayakumar, P. Sathishkumar, V. Uthayakumar, R. Chandirsekar, N. Revathi, Recent insights into the extraction, characterization, and bioactivities of chitin and chitosan from insects, Trends Food Sci. Technol. 105 (2020) 17–42, https://doi.org/10.1016/j.tifs.2020.08.016.
[55] G. Cárdenas, G. Cabrera, E. Taboada, S.P. Miranda, Chitin characterization by SEM, FTIR, XRD and ^{13}C cross polarization/mass angle spinning, J. Appl. Polym. Sci. 93 (2004) 1876–1885, https://doi.org/10.1002/app.20647.

[56] H. Kim, H. Kim, Y. Ahn, K.B. Hong, I.W. Kim, R.Y. Choi, H.J. Suh, S.H. Han, The preparation and physicochemical characterization of *Tenebrio molitor* chitin using alcalase, Molecules 28 (2023) 3254, https://doi.org/10.3390/molecules28073254.
[57] M. Rinaudo, Chitin and chitosan: properties and applications, Prog. Polym. Sci. 31 (2006) 603–632, https://doi.org/10.1016/j.progpolymsci.2006.06.001.
[58] J. Brugueroto, J. Lizardi, F.M. Goycoolea, W. Argüelles-Monal, J. Desbriers, M. Rinaudo, Amn infrared investigation in relation with chitin and chitosan characterization, Polymer 42 (2001) 3569–3580, https://doi.org/10.1016/S0032(00)00713-8.
[59] S. S. N. Machado, J. B. A. da Silva, R. Q. Nascimento, P. V. F. Lemos, D. de Jesus Assis, H. R. Marcelino, E. de Souza Ferreira, L. G. Cardoso, J. D. Pereira, J. S. Santana, M. L. A. da Silva, C. O. de Souza, Insect residues as an alternative and promising source for the extraction of chitin and chitosan, Int. J. Biol. Macromol. 254 (2024) 127773 https://doi.org/10.1016/j.ijbiomac.2023.127773.
[60] Y.S. Song, M.W. Kim, C. Moon, D.J. See, Y.S. Han, Y.H. Jo, M.Y. Noh, Y.K. Park, S. A. Kim, Y.W. Kim, W.J. Jung, Extraction of chitin and chitosan from larval exuvium and whole body of edible mealworm, *Tenebrio molitor*, Entomol. Res. 48 (2018) 227–233, https://doi.org/10.1111/1748-5967.12304.
[61] K. Mohan, S. Ravichandran, T. Muralisankar, V. Uthayakumar, R. Chandirsekar, C. Rajeevgandhi, D. Karthick Rajan, P. Seedevi, Extraction and characterization of chitin from sea snail Conus inscriptus (Reeve, Int. J. Biol. Macromol. 126 (2019) (1843) 555–560, https://doi.org/10.1016/j.ijbiomac.2018.12.241.
[62] R. Chandran, L. Williams, A. Hung, K. Nowlin, D. LaJeunesse, SEM characterization of anatomical variation in chitin organization in insect and arthropod cuticles, Micron 82 (2016) 74–85, https://doi.org/10.1016/j.micron.2015.12.010.
[63] C.Y. Soon, Y.B. Tee, C.H. Tan, A.T. Rosnita, A. Khalina, Extraction and physicochemical characterization of chitin and chitosan of *Zophobas morio* larvae in varying sodium hydroxide concentration, Int. J. Biol. Macromol. 108 (2018) 135–142, https://doi.org/10.1016/j.ijbiomac.2017.11.138.
[64] M. Triunfo, E. Tafi, A. Guarnieri, R. Salvia, C. Scienzo, T. Hahn, S. Zibek, A. Gaggliardini, L. Panariello, M.B. Coltelli, A. De Bonis, P. Fallabella, Characterization of chitin and chitosan derived from *Hermetia illucens*, a further step in a circular economy process, Sci. Rep. 12 (2022) 6613, https://doi.org/10.1038/s41598-022-10423-5.
[65] M. Kaya, S. Erdogan, A. Mol, T. Baran, Comparison of chitin structures isolated from seven *Orthoptera species*, Int. J. Biol. Macromol. 72 (2015) 797–805, https://doi.org/10.1016/j.ijbiomac.2014.09.034.
[66] H.S. Siow, K. Sudesh, P. Murugan, S. Ganesan, Mealworm (*Tenebrio molitor*) oil characterization and optimization of the free fatty acid pretreatment via acid-catalyzed esterification, Fuel 299 (2021) 120905, https://doi.org/10.1016/j.fuel.2021.120905.
[67] M. Kaya, V. Baublys, E. Can, I. Šatkauskiené, B. Bitim, V. Tubelyté, T. Baran, Comparison of physicochemical properties of chitins isolated from an insect (*Melolontha melolontha*) and a crustacean species (*Oniscus asellus*), Zoomorphology 133 (2014) 285–293, https://doi.org/10.1007/s00435-014-0227-6.